# The Histone Deacetylase Inhibitor LBH589 Is a Potent Antimyeloma Agent that Overcomes Drug Resistance

Patricia Maiso,[1] Xonia Carvajal-Vergara,[1] Enrique M. Ocio,[1,2] Ricardo López-Pérez,[1] Gema Mateo,[2] Norma Gutiérrez,[1,2] Peter Atadja,[3] Atanasio Pandiella,[1] and Jesús F. San Miguel[1,2]

[1]Centro de Investigación del Cáncer, Consejo Superior de Investigaciones Cientificas, Universidad de Salamanca; [2]Hospital Universitario de Salamanca, Salamanca, Spain; and [3]Novartis Pharmaceuticals, East Hanover, New Jersey

## Abstract

**Multiple myeloma represents an incurable disease, for which development of new therapies is required. Here, we report the effect on myeloma cells of LBH589, a new hydroxamic acid–derived histone deacetylase inhibitor. LBH589 was a potent antimyeloma agent ($IC_{50}$ < 40 nmol/L) on both cell lines and fresh cells from multiple myeloma patients, including cells resistant to conventional chemotherapeutic agents. In addition, LBH589 potentiated the action of drugs, such as bortezomib, dexamethasone, or melphalan. Using gene array, quantitative PCR, and Western analyses, we observed that LBH589 affected a large number of genes involved in cell cycle and cell death pathways. LBH589 blocked cell cycle progression, and this was accompanied by p21, p53, and p57 up-regulation. LBH589 induced cell death through an increase in the mitochondrial outer membrane permeability. LBH589 favored apoptosome formation by inducing cytochrome *c* release, Apaf-1 up-regulation, and caspase-9 cleavage. In addition, LBH589 stimulated a caspase-independent pathway through the release of AIF from the mitochondria. LBH589 down-regulated Bcl-2 and particularly Bcl-X. Moreover, overexpression of Bcl-X in multiple myeloma cells prevented LBH589-induced cell death. All these data indicate that LBH589 could be a useful drug for the treatment of multiple myeloma patients.** (Cancer Res 2006; 66(11): 5781-9)

## Introduction

New anticancer treatment strategies focus on targeting intrinsic molecular mechanisms of tumor cells, which could offer higher efficacy with less adverse effects. One of these novel anticancer family drugs, which provided promising results, are histone deacetylase (HDAC) inhibitors (1–3). Histone acetylation is presumed to be an important factor that regulates the accessibility of transcription factors to DNA (1, 2, 4). The presence of acetyl groups neutralizes the positive charges of the histones, therefore decreasing their interaction with DNA. By removing the acetyl groups, HDACs facilitate the interaction of histones with the DNA (1, 2).

Analyses on the mechanisms of HDAC inhibitor–induced cell death have indicated that these compounds may act by blocking cell cycle progression and inducing cell death (1, 2, 5). Despite the consensus on the importance of apoptosis in the effect of these drugs, the contribution of caspases to this cell death is quite controversial (5–9). In this sense, some studies have described activation of caspases (5, 7, 9, 10), whereas others advocate a caspase-independent apoptosis (6, 8). Moreover, attempts to block HDAC inhibitor–associated apoptosis with a pancaspase inhibitor (Z-VAD-FMK) have usually been ineffective (5–8), suggesting that caspase activation is not critical in HDAC inhibitor–induced apoptosis. A quite common finding in all studies has been the involvement of Bcl-2 family members in the action of HDAC inhibitor (5, 6, 8, 9, 11). Thus, cleavage of the BH3-only proapoptotic Bcl-2 family member Bid (5, 6, 8, 9), associated with mitochondrial disruption or down-regulation of Bcl-2 or Bcl-X, which act as an antiapoptotic factor, has been reported (8, 9, 11). Another mechanism proposed to be involved in the cell death caused by HDAC inhibitors has been autophagy (7).

Despite novel therapeutic strategies introduced in the treatment armamentarium of multiple myeloma, it remains an incurable disease. Therefore, new drugs are needed to improve the outcome of these patients (12). HDAC inhibitors of the hydroxamic acid family, such as SAHA (6, 13) or NVP-LAQ824 (14), have been shown to possess antimyeloma activity. However, their potency is low, as they are only effective at micromolar concentrations (6, 14). Attempts to improve the potency of HDAC inhibitor led to the development of a novel class of cynnamic acid hydroxamates that act on cells at nanomolar concentrations. One of these compounds, LBH589, has shown promising results in myeloid leukemias at low nanomolar concentrations (15). In the present study, we have analyzed the action of LBH589 on multiple myeloma cell lines and freshly isolated cells from multiple myeloma patients. Our results show that LBH589 significantly inhibited growth of multiple myeloma cells and enhanced the cytotoxicity triggered by dexamethasone, melphalan, and bortezomib. LBH589 induced cell cycle arrest and apoptosis of multiple myeloma cells, the latter involving both caspase-dependent and caspase-independent pathways. Furthermore, gene expression results uncovered a group of proteins, such as Aven (16) and Toso (17–19), which may play a relevant role in multiple myeloma apoptosis.

## Materials and Methods

**Reagents and immunochemicals.** Cell culture media, serum, and penicillin-streptomycin were from Invitrogen Corp. (Gaithersburg, MD). LBH589 was provided by Novartis Pharmaceuticals (East Hanover, NJ), and bortezomib was from Millenium Pharmaceuticals (Cambridge, MA). Annexin V-FITC was obtained from BD Biosciences (San Diego, CA). Calpeptin and Z-VAD-FMK were from Calbiochem (San Diego, CA). Other generic chemicals were purchased from Sigma Chemical Co. (St. Louis, MO), Roche Biochemicals (Mannheim, Germany), or Merck (Darmstadt, Germany).

The origins of the different antibodies employed in the Western blotting analyses were as follows: the anti-p21, anti-phospho extracellular

**Note:** P. Atadja is employed by Novartis Pharmaceuticals, Inc., the manufacturer of LBH589.

**Requests for reprints:** Atanasio Pandiella, Centro de Investigación del Cáncer, Universitad de Salamanca, Campus Miguel de Unamuno, 37007 Salamanca, Spain. Phone: 34-923-294815; E-mail: atanasio@usal.es.



doi:10.1158/0008-5472.CAN-05-4186

signal-related kinase (anti-pErk), anti-Erk1/2 anti-caspase-3 were from Santa Cruz Biotechnology (Santa Cruz, CA); the anti-Apaf-1, anti-caspase-8, anti-caspase-9, anti-cytochrome *c*, anti-AIF, anti-Bcl-X, anti-poly(ADP-ribose) polymerase (anti-PARP), anti-Bcl-2, anti-cyclin-dependent kinase 4 (anti-Cdk4), anti-cyclin D1, and anti-Bid antibodies were from BD Biosciences. The anti-p53 antibody was from Oncogene Science (Uniondale, NY). The anti-acetyl-Histone H4 was from Cell Signaling (Beverly, MA). The anti-actin antibody was from Sigma (St. Louis, MO). The horseradish peroxidase–conjugated secondary antibodies were from Bio-Rad (Richmond, CA).

**Cell cultures.** All multiple myeloma cell lines (MM1S, MM1R, U266, U266LR7, and U266DOX4) were cultured at 37°C in a humidified atmosphere in the presence of 5% $CO_2$/95% air. The source of the multiple myeloma cell lines has been described previously (20). Cell lines and bone marrow cells obtained from four multiple myeloma patients were cultured in RPMI 1640 with L-glutamine and supplemented with antibiotics (penicillin at 100 units/mL, streptomycin at 100 μg/mL) and 10% fetal bovine serum (FBS) for cell lines or 20% FBS for patient cells.

**Cell proliferation, cell cycle, and apoptosis assays.** The proliferation of multiple myeloma cells was examined using 3-(4,5-dimethylthiazol-2-yl)-2,5-diphenyltetrazolium bromide (MTT) colorimetric assays as described (20). For cell cycle analyses, the CD38-CD138/propidium iodide double-staining technique was used (21). For cytometric evaluation of apoptosis in multiple myeloma cell lines, one million MM1S cells were washed with PBS and resuspended in binding buffer [10 mmol/L HEPES/NaOH (pH 7.4), 140 mmol/L NaCl, 2.5 mmol/L $CaCl_2$]. Cells were incubated with 5 μL Annexin V-FITC for 10 minutes at room temperature in the dark, and then 10 μL propidium iodide were added. For cytometric analyses of apoptosis in bone marrow cell subpopulations from patients, the unseparated bone marrow samples were lysed and maintained in RPMI 1640 containing 20% FBS. Subsequently, the bone marrow cells were incubated with the different drugs in six-well plates during 18 hours at 37°C. To discriminate between myelomatous plasma cells and apoptotic residual bone marrow cells, we did a multiparametric technique based on the combination of Annexin V-FITC and four-color monoclonal antibodies against myeloma-associated antigens (CD38, CD56, CD28, and CD45). The use of the three first monoclonal antibodies allows the identification of plasma cells, displaying different phenotypic aberrations, whereas CD45 contributes to the identification of other hematopoietic populations. Briefly, cells were incubated for 15 minutes at room temperature in the dark with 5 μL Annexin V-FITC (Bender MedSystems, Burlingame, CA) together with a combination of monoclonal antibodies: anti-CD28-PE or anti-CD56-PE, anti-CD38-perCP/Cy5 (Cytognos, Salamanca, Spain) and anti-CD45-APC (BD Biosciences). A total of 50,000 cells were acquired on a FACSCalibur flow cytometer (BD Biosciences) and analyzed with the Paint-A-Gate program. Plasma cells were identified based on their antigenic expression, and the percentage of Annexin V–positive fraction was calculated. Simultaneously, positivity of Annexin V in $CD45^{high}$-positive cells (lymphocytes) and in $SSC^{high}$-positive, $CD38^{moderate}$-positive, and $CD45^{moderate}$-positive cells (granulocytes) was evaluated as a reference for LBH589 cytotoxicity on normal lymphocytes and granulocytes present in the same sample.

To qualitatively evaluate the mitochondrial transmembrane potential ($\Delta\Psi_m$), cells were incubated in PBS with 20 nmol/L 3,3′-dihexyloxacarbocyanine iodide [$DioC_6(3)$; Molecular Probes, Leiden, the Netherlands] for 20 minutes at 37°C, washed with PBS, and 10 μL propidium iodide (Calbiochem) were added followed by fluorescence-activated cell sorting analysis (22).

**Microarray RNA analyses.** Time course experiments carried out in MM1S cells to delineate the onset of apoptosis showed that 15 hours was sufficient to induce the early steps of apoptosis (15-20% cell death assessed by Annexin V-FITC staining). At this time point, total RNA was extracted using Trizol reagent (Life Technologies, Gaithersburg, MD) and purified with RNeasy Mini kit (Qiagen, Carlsbad, CA). The RNA integrity was assessed using Agilent 2100 Bioanalyzer (Agilent, Palo Alto, CA). Double-stranded cDNA and biotinylated cRNA were synthesized using a T7-poly-T primer and the BioArray RNA labeling kit (Enzo, Farmingdale, NY), respectively. The labeled RNA was then fragmented and hybridized to HU-133A oligonucleotide arrays (Affymetrix, Santa Clara, CA). The arrays were scanned using the Gene Array Scanner and analyzed using the DNA-Chip Analyzer (DChip). Genes with expression changes ≥2-fold in either direction were considered significant.

**Reverse transcription-PCR and quantitative PCR.** RNA isolated from MM1S cells was primed with poly-T, and cDNA was synthesized with SuperScript II RNase H-Reverse transcriptase (Invitrogen). The relative levels of gene expression were determined by real-time quantitative PCR based on a two-step SYBR green I chemistry. As a reference, we used *GAPDH*. The primers were designed using the Primer Express software (Applied Biosystems, Foster City, CA). The sequence of the primers is available upon request.

**Western blotting.** Cells were collected and centrifuged at 10,000 × *g* for 2 minutes. Then cells were washed with PBS and lysed in ice-cold lysis buffer [140 mmol/L NaCl, 10 mmol/L EDTA, 10% glycerol, 1% NP40, 20 mmol/L Tris (pH 7), 1 μmol/L pepstatin, 1 μg/mL aprotinin, 1 μg/mL leupeptin, 1 mmol/L sodium orthovanadate]. Samples were centrifuged at 10,000 × *g* at 4°C for 10 minutes, and supernatants were transferred to new tubes with the corresponding antibody and protein A-Sepharose. Immunoprecipitations and Western blotting were done as described (20).

**Subcellular fractionation.** MM1S cells were harvested in isotonic mitochondrial buffer (ref. 23; 250 mmol/L sucrose, 20 mmol/L HEPES, 10 mmol/L KCl, 1.5 mmol/L $MgCl_2$, 1 mmol/L EDTA, 1 mmol/L EGTA, 1 mmol/L DTT, 1 μmol/L pepstatin, 1 μg/mL aprotinin, 1 μg/mL leupeptin, 1 mmol/L sodium orthovanadate) and Dounce homogenized by 60 to 70 strokes. Samples were transferred to Eppendorf tubes and centrifuged at 770 × *g* for 10 minutes at 4°C to separate nuclei and unbroken cells. The resulting supernatant was centrifuged at 10,000 × *g* for 25 minutes at 4°C to obtain the mitochondrial pellet. The supernatant was further centrifuged at 100,000 × *g* for 1 hour at 4°C to yield the final soluble cytosolic fraction.

**Plasmids, generation of retroviruses, and infection.** Matrix metalloproteinase-1 (MMP-1) and MMP-1-AU1-Bcl-X were generously provided by Dr. R. Mulligan (Harvard Medical School, Boston, MA). For transient generation of retroviruses, we used a previously published protocol (20). Forty-eight hours after infection, multiple myeloma cells were analyzed for infected protein content by Western blotting.

## Results

**LBH589 induces histone acetylation in myeloma cells.** To verify whether LBH589 induced hyperacetylation of histones in myeloma, MM1S cells were treated with LBH589 for different times and concentrations of the compound, and histone H4 acetylation analyzed by Western blotting. MM1S cells exhibited a progressive increase in histone H4 acetylation correlating with the time and the dose of LBH589 (Fig. 1*A*). Treatment of MM1S cells with other compounds (melphalan, doxorubicin, and bortezomib) used in the therapy of myeloma (12, 24) indicated the specificity of the action of LBH589 on histone acetylation (Fig. 1*B*). Interestingly, melphalan and bortezomib also provoked a small increase in the acetylation of histone H4, although to a much lesser extent than LBH589.

**LBH589 is a potent antimyeloma agent and overcomes drug resistance.** To investigate the effect of LBH589 on growth and survival of multiple myeloma cells, we first used MTT assays on five different representative multiple myeloma cell lines, including sensitive and resistant to dexamethasone (MM1S and MM1R, respectively), sensitive and resistant to melphalan (U266 and U266LR7, respectively), and sensitive to doxorubicin (U266DOX4). Treatment with increasing doses of LBH589 (0.1-100 nmol/L) for 48 hours, potently suppressed MTT uptake (Fig. 1*C*). $IC_{50}$ values for these cell lines were 5.7 nmol/L (MM1S), 6.5 nmol/L (MM1R), 8.1 nmol/L (U266), 24 nmol/L (U266LR7), and 45.5 nmol/L (U266DOX4). Comparison of the $IC_{50}$ of LBH589 with other drugs

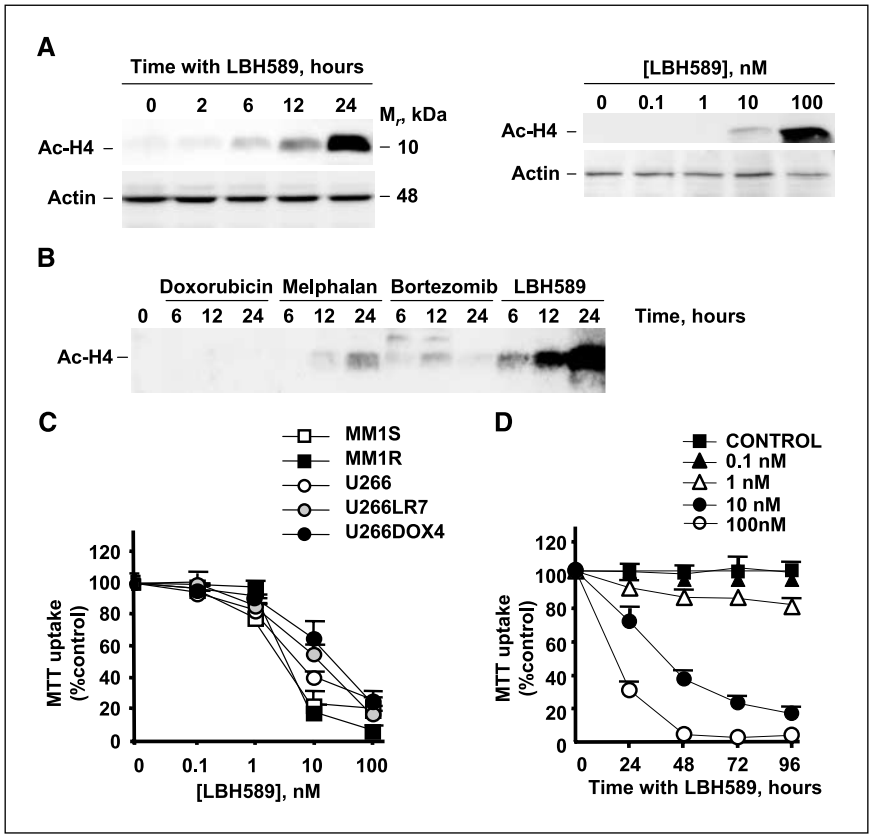


**Figure 1.** Action of LBH589 on acetylation of histone H4 in myeloma cells and on the proliferation of multiple myeloma cells. *A,* dose and time effect of LBH589 on histone H4 acetylation in myeloma cells. MM1S cells were treated for the indicated times with LBH589 (100 nmol/L; *left*) and doses for 24 hours with LBH589 (*right*), and acetylation of histone H4 was detected by Western blotting with anti-acetyl-histone H4 antibody. As a loading control, an anti-actin Western blot was done. *B,* action of different antimyeloma agents on histone H4 acetylation. Cells were treated with doxorubicin (1 μmol/L), melphalan (50 μmol/L), bortezomib (10 nmol/L), or LBH589 (100 nmol/L) for the indicated times, and acetylated histone H4 was analyzed by Western blotting. *C,* MTT uptakes of myeloma cell lines incubated with different doses of LBH589. Cells were plated at identical densities in 48-well dishes, and LBH589 was added at the indicated concentrations. MTT uptake assays were done 48 hours later as described in Materials and Methods. The average proliferation values of control untreated samples were taken as 100%. *Points,* mean of quadruplicates of an experiment that was repeated at least twice; *bars,* SD. *D,* time course and dose effect of LBH589 on MM1S cells. Cells were plated at identical densities in 48-well dishes, and LBH589 was added at the indicated concentrations. MTT uptake assays were done 24, 48, 72, and 96 hours later as described in Materials and Methods as described above.

commonly used in multiple myeloma indicated that LBH589 was slightly less potent than bortezomib ($IC_{50}$ = 2.4 nmol/L for MM1S cells) but was more potent than revlimid, dexamethasone, melphalan, doxorubicin, or arsenic trioxide (data not shown). The action of LBH589 on MM1S cells was also time dependent (Fig. 1*D*).

LBH589 was also tested on fresh bone marrow cells obtained from four multiple myeloma patients. Two of these patients (patients 1 and 2) were refractory to several lines of treatment (high-dose dexamethasone, alkylating agents and doxorubicin, and autologous stem cell transplantation, but they were not treated with bortezomib), whereas the remaining two patients (patients 3 and 4) were analyzed at diagnosis. As shown in Fig. 2*A*, all patients analyzed were sensitive to LBH589, even at the lowest dose (10 nmol/L) of the drug. Moreover, an apparent dose-response effect could be observed. One relevant finding was the low toxicity of LBH589 on the normal lymphocytes present in the same samples: no cytotoxicity was induced by LBH589 at 10 nmol/L, and only a minor increase in apoptotic cells was observed upon using 100 nmol/L of LBH589 (Fig. 2*A*). We also analyzed the effect of LBH589 on bone marrow myeloid cells. The cytotoxic effect of LBH589 on myeloid cells was slightly higher than in lymphocytes but markedly less than on malignant plasma cells (Fig. 2*A*).

**LBH589 increases the antimyeloma action of bortezomib, dexamethasone, and melphalan.** Because LBH589 acted on myeloma cells resistant to conventional antimyeloma treatments, the possibility that LBH589 could increase the action of those compounds was contemplated. To analyze this, MM1S cells were treated with combinations of LBH589 and several chemotherapeutic agents commonly used in multiple myeloma, as well as novel drugs. As shown in Fig. 2*B*, LBH589 was found to increase the antimyeloma effect of bortezomib, dexamethasone, or melphalan. However, LBH589 at concentrations as 0.1, 1, and 3 nmol/L did not enhance the ability of doxorubicin, revlimid, arsenic trioxide, or 5-aza-2′-deoxycytidine to inhibit MM1S cell proliferation (data not shown). We failed to observe any significant difference when LBH589 was added first, concomitantly, or subsequently to the other drugs (data not shown).

We also tested in fresh cells from four multiple myeloma patients the combination of LBH589 at 10 nmol/L with bortezomib (5 nmol/L). As illustrated in Fig. 2*C*, based on Annexin V staining, an additive effect was observed when LBH was combined with bortezomib compared with any of these two drugs used alone.

**LBH589 provokes cell cycle arrest in multiple myeloma cells.** The decrease in MTT uptake observed in multiple myeloma cells treated with LBH589 could be due to decreased proliferation, cell death, or both. To gain insights into the mechanism of action of LBH589 on multiple myeloma cells, we did gene expression analyses, complemented with biochemical and functional studies of cellular proteins involved in the regulation of cell cycle and survival routes.

Gene expression profiles of MM1S cells identified a total of 1,120 genes to be significantly deregulated (transcriptional changes in gene expression of ≥2-fold) by treatment with LBH589. The classification of these genes according to functional categories indicated that 9% were involved in apoptosis/responses to stress, 12% were involved in the control of cell cycle/proliferation, 18% were kinases that participate in cell cycle and survival signaling, 3% participated in adhesion, and 2% were involved in chromosome segregation/maintenance (Fig. 3*A*). These results indicated that

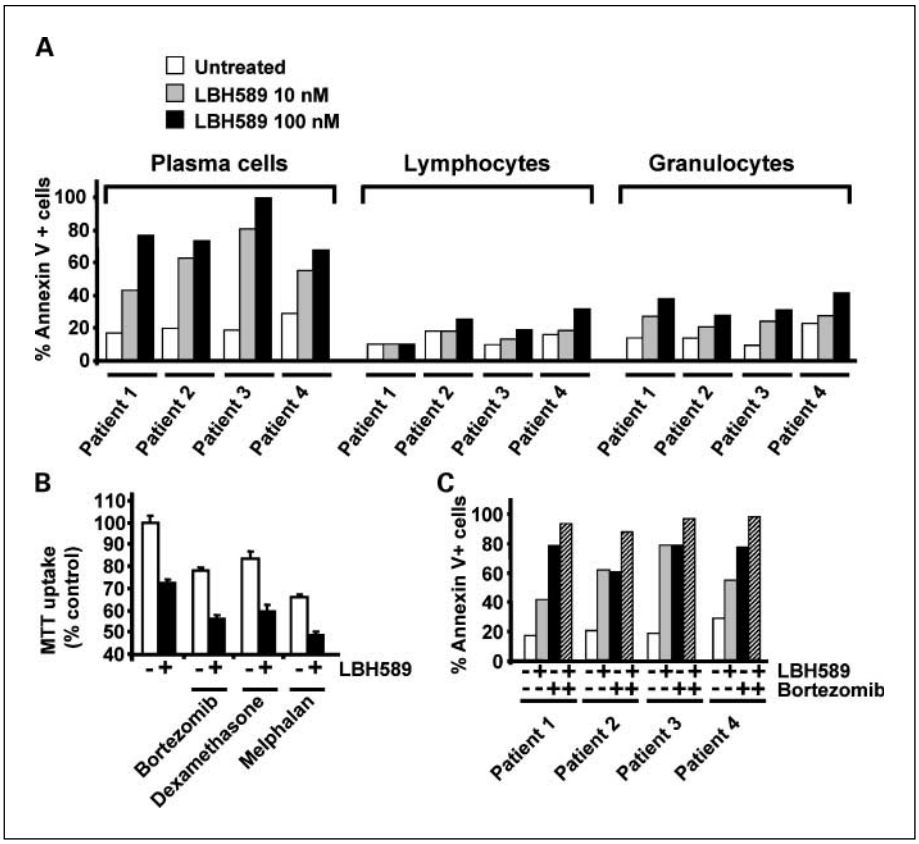


**Figure 2.** LBH589 causes death of patient cells with multiple myeloma and potentiates the antimyeloma action of bortezomib, dexamethasone, and melphalan. *A,* action of LBH589 in cells from patients with multiple myeloma. Patient cells were plated in six-well plates and treated with LBH589 at 10 and 100 nmol/L. After 18 hours, cells were stained with Annexin V-FITC and four monoclonal antibodies (CD38, CD56, CD28, and CD45), which allows the distinction between myeloma plasma cells and the remaining normal bone marrow cells, normal lymphocytes, and granulocytes. *B,* LBH589 (3 nmol/L) was combined with bortezomib (2 nmol/L), dexamethasone (1 μmol/L), or melphalan (2.5 μmol/L), and after 48 hours, MTT assays were done on MM1S cells. *C,* combination of LBH589 with bortezomib enhances cytotoxicity against patient multiple myeloma cells. Patient's multiple myeloma cells were treated with LBH589 (10 nmol/L) and bortezomib (5 nmol/L) for 18 hours, and apoptosis was determined by staining with Annexin V-FITC.

genes involved in cell cycle and cell death regulation were important targets for LBH589.

Analysis of the cell cycle distribution of MM1S cells after treatment with LBH589 showed that this drug caused an increase in $G_0$-$G_1$ and a decrease in S and $G_2$-M (Fig. 3*B*). Progression of cells into the S phase is controlled by the Cip/Kip family of cell cycle regulators p21, p27, and p57 (25). Western blotting analyses of MM1S cells treated with LBH589 for different times indicated that this compound increased the levels of p21 after 3 hours of treatment (Fig. 3*C*). The increased amount of p21 correlated with a parallel increase in p53, which transcriptionally regulates p21 levels (26). Gene expression analyses confirmed the p21 Western blotting data and, in addition, showed that LBH589 up-regulated the levels of *p57* (fold change = 6; Fig. 3*D*). Western blotting also showed that LBH589 decreased the levels of cyclin D1 and Cdk4 (Fig. 3*C*). In addition, microarray data showed that LBH589 down-regulated several other genes required for cell proliferation (*CDC25A*, *CCND2, MCM-5*, and *Ki-67*). LBH589 did not affect the phosphorylation status of Erk1/2 (Fig. 3*C*), an important route linked to multiple myeloma proliferation (27).

**LBH589 causes apoptosis in multiple myeloma cells.** Several already mentioned evidences indicated that cell death could represent an important consequence of LBH589 treatment. These include (*a*) the high number of apoptotic genes deregulated by LBH589, (*b*) the Annexin V data obtained in myeloma cells (Fig. 4*A*), and (*c*) the increase in the amount of the cells in the sub-$G_0$-$G_1$ region (from 3% to 11%). Furthermore, treatment with LBH589 caused internucleosomal DNA fragmentation, a hallmark of apoptosis (Fig. 4*B*). The degree of this effect was within the range of action of bortezomib, a potent inducer of apoptosis in multiple myeloma cells (28) that we used as a reference. As mitochondria seems to be an organelle critically involved in the triggering of apoptotic cell death (29), we explored whether LBH589 altered mitochondrial membrane potential ($\Delta\Psi_m$). Analysis of $\Delta\Psi_m$ by the use of the mitochondrial membrane potential probe $DioC_6(3)$ showed a decrease in $\Delta\Psi_m$ in cells treated with LBH589 (Fig. 4*C*).

**LBH589 causes caspase-dependent and caspase-independent cell death.** Loss of $\Delta\Psi_m$ often reflects increases in mitochondrial outer membrane permeability, which results in the release of proteins that trigger cell death (29). One of these proteins is cytochrome *c* that together with caspase-9 and Apaf-1 constitute the apoptosome, a macromolecular structure that causes activation of the effector caspase-3 (29). In addition to cytochrome *c*, increases in mitochondrial outer membrane permeability also favor the release of AIF and endonuclease G, two other mediators of apoptosis (30). Subcellular fractionation of MM1S cells treated for various times with LBH589 showed that this drug caused a time-dependent translocation of cytochrome *c* and AIF from the mitochondrial to the cytosolic fraction (Fig. 4*D*). Another component of the apoptosome (Apaf-1) was up-regulated, as determined by Western blotting (Fig. 5*A*), microarray data (fold change = 6; Fig. 5*B*), and quantitative PCR assays (Fig. 5*C*). LBH589 also caused caspase-9 and caspase-3 cleavage, with generation of active low $M_r$ cleaved fragments, as well as PARP cleavage (Fig. 5*A*).

In addition to these biochemical studies, gene expression profiling uncovered another potential regulator of the apoptosome, termed *AVEN*. This protein acts as an inhibitor of the apoptosome by inhibiting caspase-9 activation (16). *AVEN* was down regulated (fold change = −13; Fig. 5*B*) by treatment with LBH589.

Quantitative PCR analyses confirmed the decrease in *AVEN* expression, which was clearly evidenced at 12 hours (Fig. 5*C*).

The above data represented clear evidence that LBH589 triggered the activation of the intrinsic apoptotic pathway in multiple myeloma cells. To investigate the importance of this pathway in the antimyeloma action of LBH589, the ability of the caspase-3 inhibitor Z-VAD-FMK (30) to rescue from LBH589-induced cell death was evaluated. MM1S cells were preincubated for 60 minutes with Z-VAD-FMK, then LBH589 was added, and the incubations continued for 24 hours. As shown in Fig. 5*D*, preincubation with the caspase-3 inhibitor slightly blocked LBH-induced cell death. In contrast, Z-VAD-FMK had a much higher inhibitory effect on the cell death caused by bortezomib, as previously described (31). These results indicated that although LBH589 activated the caspase-dependent apoptotic pathway; this activation was not the sole executor of cell death caused by this compound.

Other HDAC inhibitors, such as SAHA, have been shown to cause apoptotic cell death through caspase-independent routes (6). These alternative routes include mitochondrial release of the above mentioned proapoptotic factors AIF and endonuclease G, or activation of calcium-dependent proteases, such as calpain (30). To evaluate a potential role of calpain in the action of LBH589, MM1S cells were incubated with the calpain inhibitor calpeptin (50 nmol/L), and its effect on LBH589-induced cell death was analyzed at different times (24, 36, 48 hours). Calpeptin was unable to prevent LBH589-induced cell death, indicating that this effect of LBH589 does not involve activation of calpain (data not shown).

**Action of LBH589 on the extrinsic apoptotic pathway.** Recent reports have suggested that HDAC inhibitors may act through up-regulation of receptors and ligands of the Fas or tumor necrosis factor–related apoptosis-inducing ligand (TRAIL) family, which are linked to the activation of the extrinsic apoptotic pathway (30). Treatment of MM1S cells with LBH589 failed to reveal substantial changes in the levels of Fas or its ligand, TRAIL, or its receptors (Fig. 5*B* and *E*; data not shown). Interestingly, however, the gene expression analyses identified a gene, termed *TOSO*, which showed a marked down-regulation (fold change = −90). This effect of LBH589 was confirmed by quantitative PCR

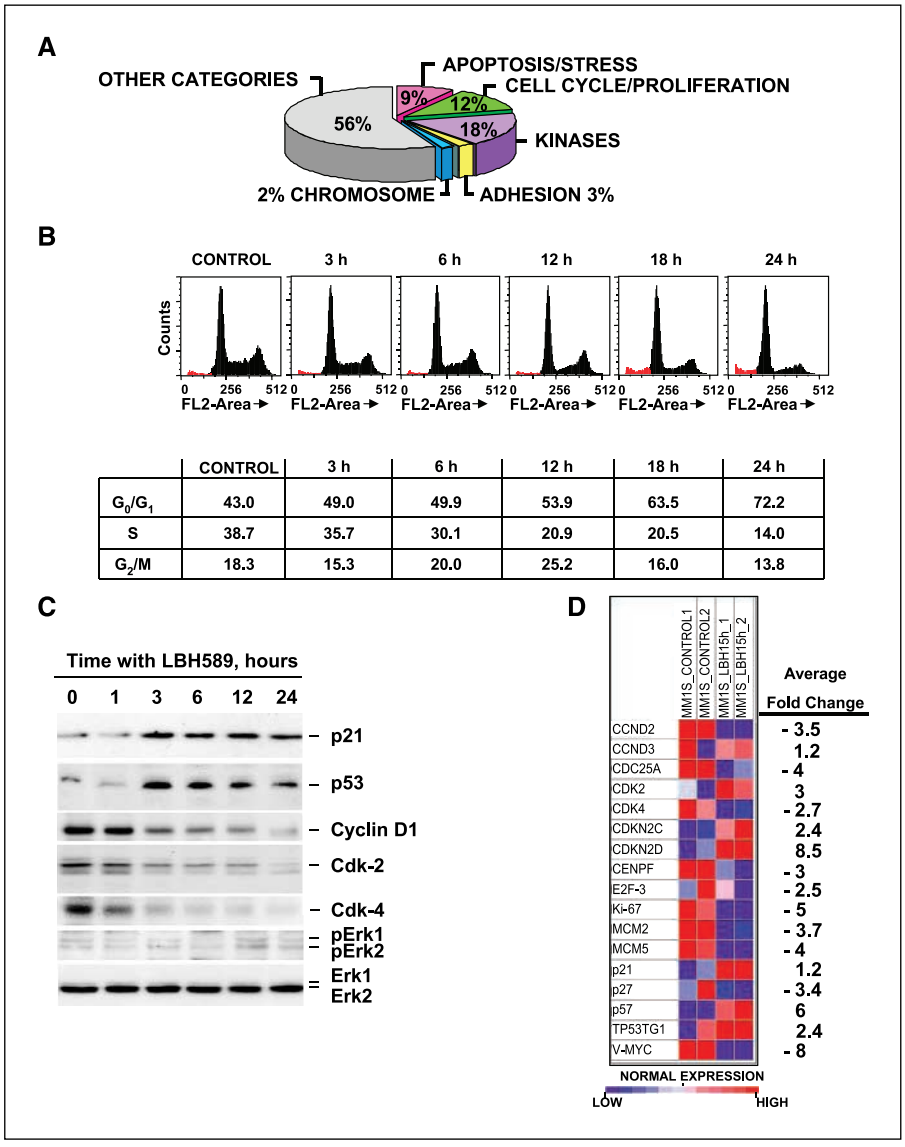


| | CONTROL | 3 h | 6 h | 12 h | 18 h | 24 h |
|---|---|---|---|---|---|---|
| $G_0/G_1$ | 43.0 | 49.0 | 49.9 | 53.9 | 63.5 | 72.2 |
| S | 38.7 | 35.7 | 30.1 | 20.9 | 20.5 | 14.0 |
| $G_2/M$ | 18.3 | 15.3 | 20.0 | 25.2 | 16.0 | 13.8 |

**Figure 3.** *A,* genes deregulated by LBH589. MM1S cells were treated with LBH589 (100 nmol/L). RNA was isolated, and cDNA was hybridized to oligonucleotide microarrays and incubated as described in Materials and Methods. Genes modified ≥2-fold were grouped according to different functional categories. *B,* LBH589 causes cell cycle changes in MM1S cells. MM1S cells were incubated with LBH589 (100 nmol/L) for 3, 6, 12, 18, and 24 hours and examined for cell cycle profile using CD38-CD138/propidium iodide double staining. Bottom, percentage of cells in the different cell cycle phases. *C,* MM1S cell were treated with LBH589 (100 nmol/L) for the indicated times, and the expression of cell cycle–related proteins was analyzed by Western blotting. *D,* colorgram of cell cycle deregulated genes after 15 hours of LBH589 (100 nmol/L) treatment. Results from two different experiments (Control_1 versus LBH15h_1 and Control_2 versus LBH15h_2). Average fold change for both experiments (*right*).

(Fig. 5*E*). Toso has formerly been reported to negatively regulate FAS- or TRAIL-induced apoptosis in other cell types (17, 18), and its amount decreases also in myeloma cells treated with bortezomib (32).

As far as caspases are involved in the extrinsic apoptotic pathway, LBH589 provoked caspase-8 cleavage with generation of truncated fragments (Fig. 5*F*). In addition, cleavage of Bid with generation of its proapoptotic truncated form was also evidenced although at later times of LBH589 exposure (Fig. 5*F*).

**Overexpression of Bcl-X impairs LBH589-induced cell death.** Bcl-2 family members act as important regulators of mitochondrial outer membrane permeability (30). Microarray analyses indicated that LBH589 down regulated the Bcl-2 family members *BCL2* (fold change = −2) and particularly *BCLX* (fold change = −170; Fig. 5*B*). Both Western blotting (Fig. 6*A*) and quantitative PCR (Fig. 5*C*) confirmed these results. Because Bcl-X displayed the higher gene disregulation, the possibility that restoration of its levels could affect LBH589 efficacy was analyzed. To this end, MM1S cells were infected with a retroviral vector that coded for an AU1 epitope-tagged version of Bcl-X. As shown in Fig. 6*B*, inclusion of the AU1 tag caused a retardation in the $M_r$ of AU1-Bcl-X, which allowed distinction from autoctonous Bcl-X. MM1S cells expressing AU1-Bcl-X, in addition to endogenous Bcl-X, were more resistant to cell death than MM1S cells infected with the empty vector (Fig. 6*C*).

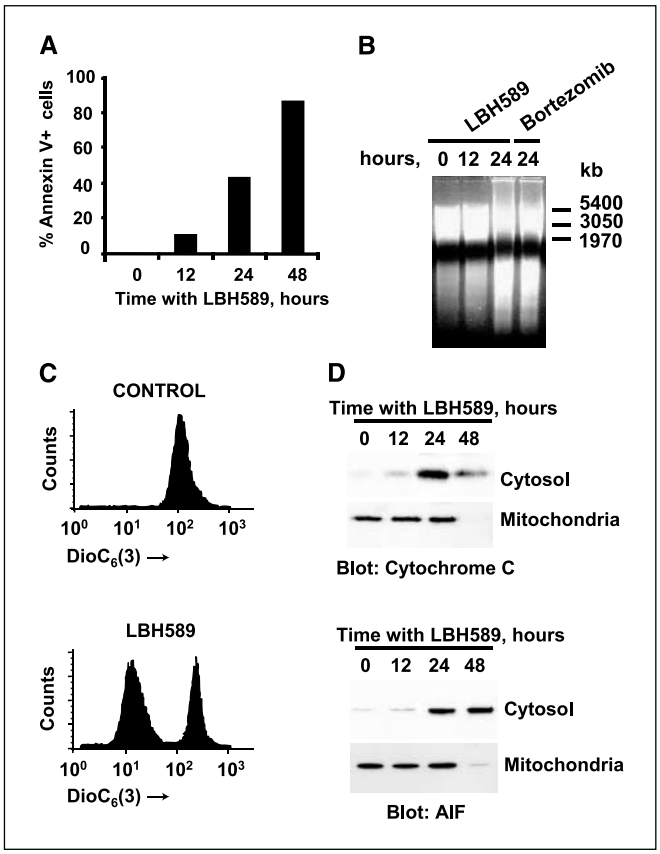


**Figure 4.** LBH589 disrupts the mithochondrial outer membrane and causes apoptosis. *A,* time course experiment with LBH589 showing increasing cell death (Annexin-positive cells). *B,* LBH589 provokes DNA fragmentation. MM1S cells were treated with LBH589 (100 nmol/L) or bortezomib (10 nmol/L) for the indicated times, and DNA was isolated and analyzed by agarose gel electrophoresis. Position of the $M_r$ markers (*right*). *C,* LBH589 induces $\Delta\Psi_m$ disruption. MM1S cells were treated with LBH589 (100 nmol/L), and the $\Delta\Psi_m$ analyses were done with [$DiOC_6(3)^{low}$] by flow cytometry. *D,* MM1S were treated for the indicated times with LBH589, and the subcellular distribution of cytochrome *c* and AIF in mithochondrial and cytosolic fractions was analyzed by Western blotting.

## Discussion

HDAC inhibitors are a novel class of chemotherapeutic agents identified by their ability to induce apoptosis and inhibit the cell cycle (1, 2). We evaluated the effects of HDAC inhibition by LBH589 in cell lines and fresh tumor cells from patients with multiple myeloma. The effect of LBH589 on multiple myeloma cell lines was observed at an $IC_{50}$ in the low nmol/L range, close to that of bortezomib, and significantly lower than that observed for dexamethasone, melphalan, doxorubicin, revlimid, and arsenic trioxide. This efficacy is superior to that of the related HDAC inhibitors SAHA (6, 13) and NVP-LAQ824 (14), whose action on myeloma cells occurs at micromolar concentrations. Moreover, LBH589 synergized with bortezomib, dexamethasone, and melphalan to decrease multiple myeloma cell number. In addition, analyses of apoptosis on fresh tumor cells from multiple myeloma patients showed that LBH589 had a similar antimyeloma activity to that found on multiple myeloma cell lines, and this was observed not only on plasma cells from untreated patients but also on patients with refractory disease. Moreover, using a multiparametric flow cytometry approach, which allows the discrimination between myelomatous plasma cells and residual normal bone marrow cells, we observed that LBH589 cytotoxicity was very selective for tumor cells because only marginally affected bone marrow lymphocytes or granulocytes. Taken together, these data show that LBH589 has potent *in vitro* antimyeloma activity. Furthermore, the observed synergistic interaction between LBH589 and other antimyeloma compounds may translate into attractive combinations in the clinical setting.

Our studies on the mechanism of action of LBH589 indicate that this compound affects several routes involved in the control of cell cycle progression and apoptosis. LBH589 caused a progressive accumulation of cells in $G_0$-$G_1$ phases with a decrease in the percentage of cells in proliferative phases (S and $G_2$-M) in MM1S cells. Western blotting and microarray analyses indicated changes in the amounts of the Cip/Kip family of cell cycle regulators p21, p27, and p57. LBH589 caused an increase in the amount of p21. Induction of p21 has previously been shown to occur in multiple myeloma cells treated with other HDAC inhibitor, such as depsipeptide (11), NVP-LAQ824 (14), or SAHA (6, 13). Furthermore, p21 increases have been reported in leukemia cells treated with LBH589 (15). In addition, LBH589 also increased the levels of p53, an upstream transcriptional regulator of p21, and also increased p57 expression, a Cip/Kip family protein that arrests the cell cycle (33).

In addition to its effect on the cell cycle, LBH589 provoked cell death. Criteria for the latter include Annexin V positivity, an increase in the sub-$G_0$ region in cytometry studies, and DNA fragmentation. Analyses of the effect of LBH589 on multiple myeloma cells indicated that this compound caused cell death through mitochondrial perturbation. Progressive loss of the mitochondrial membrane potential reflected an increase in the permeability of the outer mitochondrial membrane, which allowed release of proapoptotic proteins, such as cytochrome *c* or AIF. The former, together with caspase-9 and Apaf-1, interacts to create the apoptosome (29, 30). We have observed by oligonucleotide arrays,

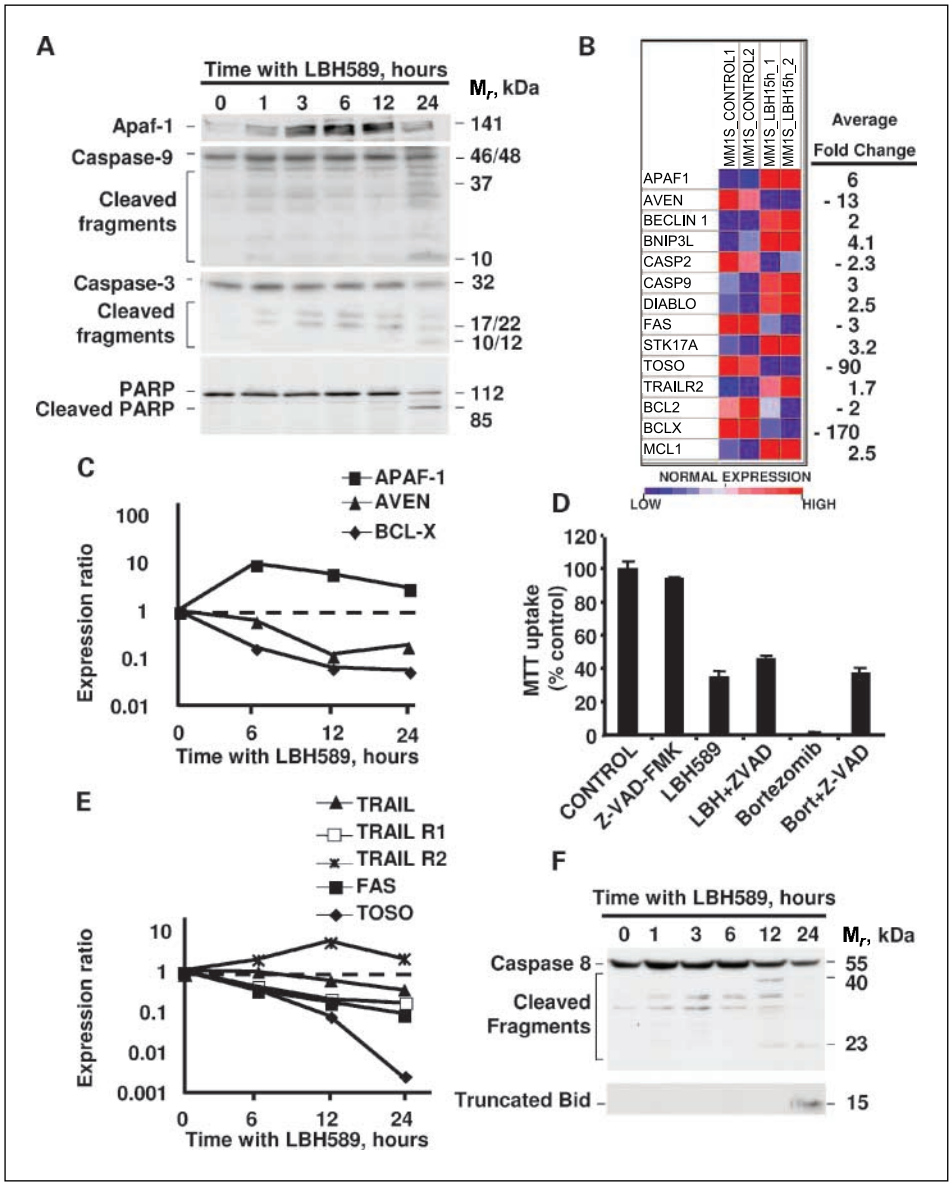


**Figure 5.** Effect of LBH589 on apoptotic pathways. *A,* MM1S cells were treated with LBH589 (100 nmol/L) for the indicated times, and expression of Apaf-1, caspase-9, caspase-3, and PARP proteins was analyzed by Western blotting of cell extracts using specific antibodies. *B,* colorgram of genes involved in apoptosis deregulated after 15 hours of LBH589 (100 nmol/L) treatment. *C,* validation of microarray data by SYBR Green quantitative real-time PCR. Values for each gene were normalized to expression levels of *GAPDH*. From an experiment representative of at least three independent experiments. *D,* effect of the pancaspase inhibitor Z-VAD-FMK on LBH589-induced cell death. MM1S cells were plated and pretreated where indicated, with Z-VAD-FMK (50 μmol/L) for 60 minutes. LBH589 (100 nmol/L) or bortezomib (10 nmol/L) were added to the corresponding samples, and the experiment was continued for 24 hours. MTT uptake was carried out as described above. *E,* gene expression data obtained by quantitative PCR analyses of five genes that participate in the extrinsic apoptotic pathway. Representative of at least three independent experiments. *F,* activation of caspase-8 and cleavage of Bid induced by LBH589. MM1S cells were treated as in (*A*), and the cleavage of caspase-8 and Bid was examined by Western blotting.

reverse transcription-PCR, and Western blotting a significant increase in Apaf-1 expression following LBH589 treatment. In addition, LBH589 provoked caspase-9 activation/cleavage. In line with our observations, Mitsiades et al. (13) have also shown that Apaf-1 is up-regulated in multiple myeloma cells treated with SAHA. Recent elegant studies showing that SAHA-induced cell death can be prevented by Apaf-1 knock down add further evidence on the role of Apaf-1 in the mechanism of action of HDAC inhibitors (34). Microarray analyses, confirmed by quantitative PCR, identified another protein (Aven) that may participate in the regulation of the apoptosome. Aven, which binds to Apaf-1 (16), has been shown to interfere with the ability of Apaf-1 to induce activation of caspases. Exposure of MM1S cells to LBH589 decreased the amount of Aven, potentially favoring the proapoptotic action of Apaf-1.

As expected from its action on the apoptosome, LBH589 caused cleavage of the effector caspase-3, that in turn provoked PARP cleavage. This latter effect was supported by the blockade of PARP cleavage in cells preincubated with Z-VAD-FMK before the addition of LBH589.[4] This is in contrast to SAHA that did not activate caspase-3, caspase-8, or caspase-9 in multiple myeloma cells (6). Both LBH589 and SAHA induced PARP cleavage in multiple myeloma cells. However, whereas the former compound produced an 85-kDa fragment, SAHA generated an atypical 60-kDa fragment (6). Moreover, pretreatment with the calpain inhibitor calpeptin did not reduce LBH589-induced apoptosis, whereas it protected against SAHA-induced apoptosis (6). Furthermore, although activation of caspases is involved in apoptosis, in the case of LBH589, other mechanisms are required because pretreatment with the wide range caspase inhibitor Z-VAD-FMK only slightly reduced apoptosis. It is also possible that the failure of Z-VAD-FMK to prevent LBH589-induced cell death may be due to a high degree of mitochondrial derangement, which is upstream of caspase activation (30). Therefore, the mechanism of cell death by

[4] X. Carvajal-Vergara and A. Pandiella, unpublished data.

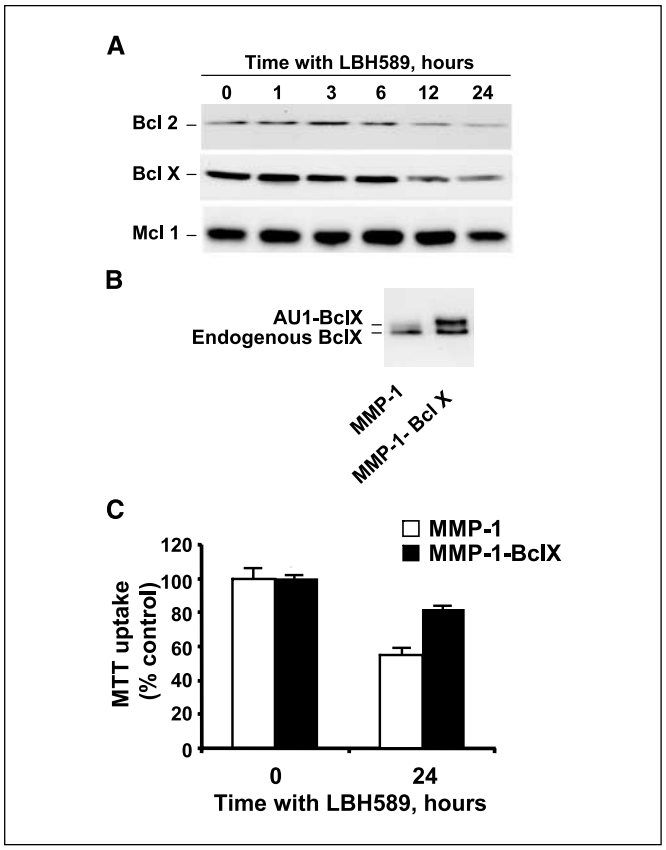


**Figure 6.** Expression of Bcl-X prevents LBH589-induced cell death. *A,* action of LBH589 on the levels of Bcl-2 and Bcl-X proteins. MM1S cells were treated with LBH589 (100 nmol/L) for the indicated times, and cell extracts were used for Western blotting with anti-Bcl-2 and anti-Bcl-X antibodies. *B,* expression of wild-type AU1-Bcl-X in MM1S cells. Cells were infected with retroviruses that included an empty vector, or an AU1-Bcl-X containing vector, and the expression of the exogenous and endogenous Bcl-X protein was analyzed by Western blotting of cell extracts with an anti-Bcl-X antibody. *C,* action of AU1-Bcl-X expression on LBH589-induced cell death. Control and AU1-Bcl-X-expressing MM1S cells were plated at identical densities, and then LBH589 was added, where indicated. Cell viability was analyzed 24 hours later by MTT assays as described above. *Columns,* mean of quadruplicates; *bars,* SD.

LBH589 seems different from that of SAHA, which is calpain dependent and caspase independent.

Recent studies have shown that AIF, together with endonuclease G, mediates cell death through a caspase-independent pathway (30). AIF translocates from the mitochondria to the cytosol, in transit to the nucleus, where it interacts with DNA and stimulates, together with endonuclease G, the formation of the degradosome (30). The latter complex mediates chromatin condensation, proteolysis, and DNA damage. We have shown that LBH589 induces translocation of AIF from the mitochondria to the cytosolic fraction, and this was concomitant with the release of cytochrome *c* to the cytosol. These data suggest that release of AIF may play a relevant role in cell death induced by LBH589.

Bcl-2 family members have been shown to regulate mitochondrial outer membrane permeability (29, 30). Western blotting, quantitative PCR, and microarray studies indicated that LBH589 down-regulated the antiapoptotic proteins Bcl-2 and Bcl-X. These data are in line with the down-regulation of the expression of Bcl-2 and Bcl-X reported with depsipeptide in multiple myeloma cell lines (11) and SAHA (6) in myeloma cells. In addition to the biochemical data, functional evidence indicated the important role of the interplay of Bcl-2 family members and mitochondria in the action of LBH589. Thus, when MM1S cells were infected with a retrovirus that coded for an epitope-tagged form of Bcl-X, therefore increasing the total amount of cellular Bcl-X, the apoptotic action of LBH589 was profoundly compromised.

In conclusion, LBH represents a novel hydroxamic acid–derived HDAC inhibitor with strong activity against multiple myeloma at nanomolar concentrations. LBH induced growth arrest and caspase-dependent and caspase-independent apoptosis. The action of LBH589 on resistant multiple myeloma cell lines and on fresh plasma cells from patients with refractory disease, together with its capacity to potentiate other anti-myeloma agents, would support the clinical evaluation of LBH589 in multiple myeloma.

## Acknowledgments

Received 11/23/2005; revised 1/18/2006; accepted 3/27/2006.

**Grant support:** Spanish Association Against Cancer (A. Pandiella and J. San Miguel), International Myeloma Foundation (A. Pandiella and J. San Miguel), FISS-FEDER (A. Pandiella and J. San Miguel), Spanish Myeloma Network Program G03/136, Glaxo-Consejo Superior de Investigaciones Cientificas fellowship (X. Carvajal-Vergara), Plan Nacional de Investigación Científica, Desarrollo e Innovación Tecnológica (I+D+I; E.M. Ocio), and Instituto de Salud Carlos III-Fondo de Investigación Sanitaria with expedient no. 400001 (E.M. Ocio).

The costs of publication of this article were defrayed in part by the payment of page charges. This article must therefore be hereby marked *advertisement* in accordance with 18 U.S.C. Section 1734 solely to indicate this fact.

We thank Sheila Mateos-Domínguez for excellent technical assistance.

## References

1. Miller TA, Witter DJ, Belvedere S. Histone deacetylase inhibitors. J Med Chem 2003;46:5097–116.
2. Drummond DC, Noble CO, Kirpotin DB, Guo Z, Scott GK, Benz CC. Clinical development of histone deacetylase inhibitors as anticancer agents. Annu Rev Pharmacol Toxicol 2005;45:495–528.
3. Marks P, Rifkind RA, Richon VM, Breslow R, Miller T, Kelly WK. Histone deacetylases and cancer: causes and therapies. Nat Rev Cancer 2001;1:194–202.
4. Yang XJ, Gregoire S. Class II histone deacetylases: from sequence to function, regulation, and clinical implication. Mol Cell Biol 2005;25:2873–84.
5. Peart MJ, Tainton KM, Ruefli AA, et al. Novel mechanisms of apoptosis induced by histone deacetylase inhibitors. Cancer Res 2003;63:4460–71.
6. Mitsiades N, Mitsiades CS, Richardson PG, et al. Molecular sequelae of histone deacetylase inhibition in human malignant B cells. Blood 2003;101:4055–62.
7. Shao Y, Gao Z, Marks PA, Jiang X. Apoptotic and autophagic cell death induced by histone deacetylase inhibitors. Proc Natl Acad Sci U S A 2004;101:18030–5.
8. Ruefli AA, Ausserlechner MJ, Bernhard D, et al. The histone deacetylase inhibitor and chemotherapeutic agent suberoylanilide hydroxamic acid (SAHA) induces a cell-death pathway characterized by cleavage of Bid and production of reactive oxygen species. Proc Natl Acad Sci U S A 2001;98:10833–8.
9. Henderson C, Mizzau M, Paroni G, Maestro R, Schneider C, Brancolini C. Role of caspases, Bid, and p53 in the apoptotic response triggered by histone deacetylase inhibitors trichostatin-A (TSA) and suberoylanilide hydroxamic acid (SAHA). J Biol Chem 2003;278:12579–89.
10. Amin HM, Saeed S, Alkan S. Histone deacetylase inhibitors induce caspase-dependent apoptosis and downregulation of daxx in acute promyelocytic leukaemia with t(15;17). Br J Haematol 2001;115:287–97.
11. Khan SB, Maududi T, Barton K, Ayers J, Alkan S. Analysis of histone deacetylase inhibitor, depsipeptide (FR901228), effect on multiple myeloma. Br J Haematol 2004;125:156–61.
12. Anderson KC. Moving disease biology from the lab to the clinic. Cancer 2003;97:796–801.
13. Mitsiades CS, Mitsiades NS, McMullan CJ, et al. Transcriptional signature of histone deacetylase inhibition in multiple myeloma: biological and clinical implications. Proc Natl Acad Sci U S A 2004;101:540–5.
14. Catley L, Weisberg E, Tai YT, et al. NVP-LAQ824 is a potent novel histone deacetylase inhibitor with significant activity against multiple myeloma. Blood 2003;102:2615–22.

15. George P, Bali P, Annavarapu S, et al. Combination of the histone deacetylase inhibitor LBH589 and the hsp90 inhibitor 17-AAG is highly active against human CML-BC cells and AML cells with activating mutation of FLT-3. Blood 2005;105:1768–76.
16. Chau BN, Cheng EH, Kerr DA, Hardwick JM. Aven, a novel inhibitor of caspase activation, binds Bcl-xL and Apaf-1. Mol Cell 2000;6:31–40.
17. Hitoshi Y, Lorens J, Kitada SI, et al. Toso, a cell surface, specific regulator of Fas-induced apoptosis in T cells. Immunity 1998;8:461–71.
18. Song Y, Jacob CO. The mouse cell surface protein TOSO regulates Fas/Fas ligand-induced apoptosis through its binding to Fas-associated death domain. J Biol Chem 2005;280:9618–26.
19. Shiiki K, Yoshikawa H, Kinoshita H, et al. Potential mechanisms of resistance to TRAIL/Apo2L-induced apoptosis in human promyelocytic leukemia HL-60 cells during granulocytic differentiation. Cell Death Differ 2000;7:939–46.
20. Carvajal-Vergara X, Tabera S, Montero JC, et al. Multifunctional role of Erk5 in multiple myeloma. Blood 2005;105:4492–9.
21. Orfao A, Garcia-Sanz R, Lopez-Berges MC, et al. A new method for the analysis of plasma cell DNA content in multiple myeloma samples using a CD38/propidium iodide double staining technique. Cytometry 1994;17: 332–9.
22. Gajate C, Santos-Beneit AM, Macho A, et al. Involvement of mitochondria and caspase-3 in ET-18-OCH(3)-induced apoptosis of human leukemic cells. Int J Cancer 2000;86:208–18.
23. Hockenbery D, Nunez G, Milliman C, Schreiber RD, Korsmeyer SJ. Bcl-2 is an inner mitochondrial membrane protein that blocks programmed cell death. Nature 1990;348:334–6.
24. Mitsiades CS, Mitsiades N, Munshi NC, Anderson KC. Focus on multiple myeloma. Cancer Cell 2004;6: 439–44.
25. Malumbres M, Hunt SL, Sotillo R, et al. Driving the cell cycle to cancer. Adv Exp Med Biol 2003;532:1–11.
26. Gartel AL,Tyner AL. Transcriptional regulation of the p21((WAF1/CIP1)) gene. Exp Cell Res 1999;246:280–9.
27. Ogata A, Chauhan D, Teoh G, et al. IL-6 triggers cell growth via the Ras-dependent mitogen-activated protein kinase cascade. J Immunol 1997;159:2212–21.
28. Hideshima T, Richardson P, Chauhan D, et al. The proteasome inhibitor PS-341 inhibits growth, induces apoptosis, and overcomes drug resistance in human multiple myeloma cells. Cancer Res 2001;61:3071–6.
29. Danial NN, Korsmeyer SJ. Cell death: critical control points. Cell 2004;116:205–19.
30. Kroemer G, Martin SJ. Caspase-independent cell death. Nat Med 2005;11:725–30.
31. Hideshima T, Chauhan D, Hayashi T, et al. Proteasome inhibitor PS-341 abrogates IL-6 triggered signaling cascades via caspase-dependent downregulation of gp130 in multiple myeloma. Oncogene 2003;22:8386–93.
32. Mitsiades N, Mitsiades CS, Poulaki V, et al. Molecular sequelae of proteasome inhibition in human multiple myeloma cells. Proc Natl Acad Sci U S A 2002; 99:14374–9.
33. Sherr CJ, Roberts JM. CDK inhibitors: positive and negative regulators of $G_1$-phase progression. Genes Dev 1999;13:1501–12.
34. Peart MJ, Smyth GK, van Laar RK, et al. Identification and functional significance of genes regulated by structurally different histone deacetylase inhibitors. Proc Natl Acad Sci U S A 2005;102:3697–702.